

Phosphoryl Group as a Strong σ -Donor Anionic Phosphine-Type Ligand: A Combined Experimental and Theoretical Study on Long-Lived Room Temperature Luminescence of the $[\text{Ru}(\text{tpy})(\text{bpy})(\text{Ph}_2\text{PO})]^+$ Complex

Emilie Lebon,^{†,‡} Rémy Sylvain,^{†,‡} Rémi E. Piau,[§] Cloé Lanthony,[§] Julien Pilmé,^{⊥,¶} Pierre Sutra,^{†,‡} Martial Boggio-Pasqua,[§] Jean-Louis Heully,[§] Fabienne Alary,^{*,§} Alberto Juris,^{||} and Alain Igau^{*,†,‡}

[†]Laboratoire de Chimie de Coordination, CNRS, 205 route de Narbonne, 31077 Toulouse, France

[‡]Université de Toulouse, UPS, INPT, 31077 Toulouse, France

[§]Laboratoire de Chimie et Physique Quantiques, UMR 5626, IRSAMC, CNRS et Université de Toulouse, 31077 Toulouse, France

^{||}Dipartimento di Chimica "G. Ciamician" Università di Bologna, via Selmi 2, 40126 Bologna, Italy

[⊥]Laboratoire de Chimie Théorique, Sorbonne Universités, UPMC, Université Paris 06, UMR 7616, F-75005 Paris, France

[¶]Laboratoire de Chimie Théorique, UMR 7616, CNRS, F-75005 Paris, France

Supporting Information

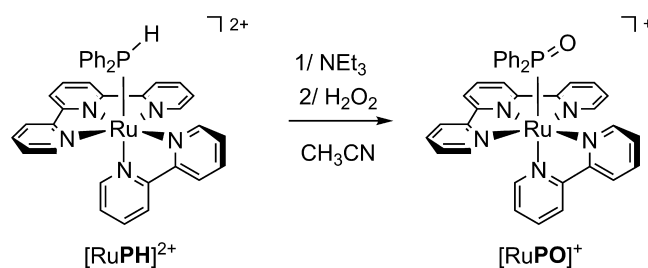
ABSTRACT: A phosphoryl Ru(II) polypyridyl complex was prepared in a one-pot process. Theoretical analysis suggests that the phosphoryl ligand may be viewed as a strong σ -donor anionic phosphine L-type ligand. State-of-the-art free-energy profile calculations on the excited states demonstrate that both favorable thermodynamic and kinetic factors are responsible for the remarkable room temperature luminescence properties of the phosphoryl complex.

Because of their unique properties in terms of absorbance in the visible range, chemical stability, excited-state lifetimes, and favorable redox potentials in the excited state that can be fine-tuned by the adjacent ligands, ruthenium polypyridine complexes¹ have found notable applications in current organic electronics.² We recently demonstrated that suitable functionalization of largely neglected organophosphorus ligands can promote room temperature luminescence of $[\text{Ru}(\text{tpy})(\text{bpy})\text{L}]^{2+}$ species.³ Recent research has shown that the incorporation of a phosphoryl unit, $-\text{P}(\text{O})\text{R}_2$, can be used to tailor the HOMO/LUMO levels of conjugated systems.⁴ Inspired by these results, we decided to coordinate the phosphoryl unit $-\text{P}(\text{O})\text{R}_2$ on the $[\text{Ru}(\text{tpy})(\text{bpy})]^{2+}$ metal core. We anticipated that such a ligand would have major consequences on the electrochemical and optical properties of these species by destabilizing the non-emissive metal-centered triplet state (³MC) relative to the triplet metal-to-ligand charge-transfer excited state (³MLCT), known to be responsible for luminescence. This is investigated therein by density functional theory (DFT) calculations. Moreover, the nature of the phosphoryl PO bond has been the subject of intense studies for many years.^{5,6} As a complementary study, we also report theoretical investigations on the PO and RuP bonding scheme of the P-metalated phosphoryl moiety $-\text{P}(\text{O})\text{R}_2$.

We prepared in a one-pot process, starting from the secondary phosphine complex $[\text{RuPH}]^{2+}$ (with $\text{P} = \text{PPh}_2$) and following the

deprotonation/oxidation sequence, the phosphoryl $[\text{RuPO}]^+$ complex isolated in 92% yield as a red solid (Scheme 1).

Scheme 1. Synthesis of the Phosphoryl $[\text{RuPO}]^+$ Complex from $[\text{RuPH}]^{2+}$ ($\text{P} = \text{PPh}_2$ and PF_6^- as Counteranions)



$[\text{RuPO}]^+$ has been fully characterized by a combination of spectroscopic techniques. ³¹P NMR showed the disappearance of the chemical shift for $[\text{RuPH}]^{2+}$ at 32.9 ppm with a ¹J_{PH} coupling constant of 365.0 Hz, characteristic of secondary phosphine coordinated on a metal fragment, at the expense of a single signal at 80.0 ppm. Mass spectrometry analyses allowed us to identify the molecular $[\text{M} - \text{PF}_6]^+$ peak for $[\text{RuPO}]^+$.

The nature of the phosphoryl–ruthenium bond in $[\text{RuPO}]^+$ was investigated using electron localization function (ELF)⁷ and natural bond orbital (NBO)⁸ analysis (Figure 1). The population of the ELF basin $V(\text{Ru},\text{P}) = 2.20$ electrons lies in the range for dative metal–phosphine bonds.⁹ The oxygen atom of the phosphoryl moiety exhibits a strong anionic character, as indicated by its negative charge from natural population analysis (−1.22) and its population of the ELF valence basin (5.96 electrons). As already proposed by Kirchner et al.,⁶ our theoretical study clearly suggests that the phosphoryl ligand can be better represented by the canonical structure (B)

Received: November 18, 2013

Published: January 28, 2014

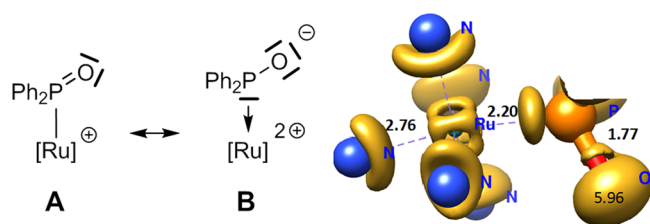


Figure 1. Two extreme canonical structures (left) and bonding description of the P-metalated phosphoryl ligand in $[\text{RuPO}]^+$ (right). The isosurfaces around the ruthenium atom correspond to the ELF value of 0.8. The numbers are the population of selected ELF basins. Aryl substituents have been deleted for clarity.

corresponding to an L-type phosphine ligand with an anionic charge centered on the oxygen atom featuring a P–Ru dative bond with one lone pair of electrons at the phosphorus atom rather than the resonance form (A) widely used in the literature.

The electronic properties of $[\text{RuPH}]^{2+}$ and $[\text{RuPO}]^+$ were probed using cyclic and square-wave voltammetries. For $[\text{RuPH}]^{2+}$, the irreversible first oxidation and quasi-reversible first reduction processes were respectively observed at +1.40 and -1.25 V/ECS; these values are fully comparable to those previously reported for $[\text{RuPPh}]^{2+}$.³ The oxidation and reduction irreversible processes of $[\text{RuPO}]^+$ are registered respectively at +0.94 and -1.35 V/ECS. The oxidation potential of $[\text{RuPO}]^+$ is the lowest reported to date for a $[\text{Ru}(\text{tpy})(\text{bpy})]^{2+}$ fragment with a phosphorus ligand coordinated to the metal core and decreased significantly by 470 mV from that registered for the precursor $[\text{RuPH}]^{2+}$ (Figure 2).

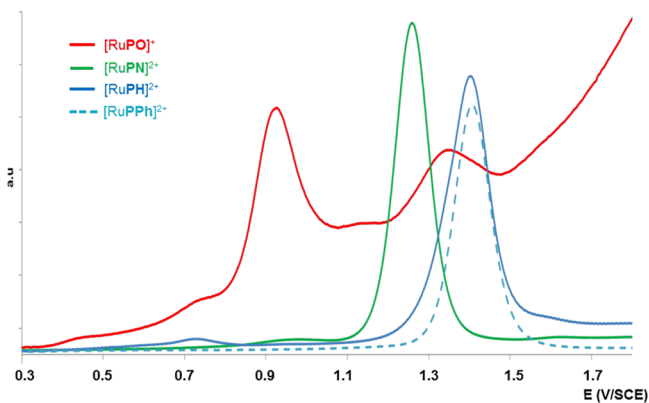


Figure 2. Oxidation potentials of the $[\text{RuPPh}]^{2+}$,³ $[\text{RuPH}]^{2+}$, $[\text{RuPO}]^+$, and $[\text{RuP}(\text{N})]^{2+}$ complexes (P = PPh_2 and (N) = $\text{N}=\text{C}(\text{H})\text{N}(\text{i-Pr})_2$ and PF_6^- as counteranions).

DFT calculations¹⁰ show that, in all cases, the HOMO is essentially a metallic orbital and the LUMO is a π^* orbital localized on the tpy ligand, implying a Ru-based oxidation and a tpy-based reduction. Destabilization of the HOMO in $[\text{RuPO}]^+$ is caused by the low π -acceptor ability of the phosphoryl PO ligand with respect to the PH ligand (-6.94 and -7.56 eV, respectively).

The UV/vis absorption spectra of $[\text{RuPH}]^{2+}$, $[\text{RuP}(\text{N})]^{2+}$, and $[\text{RuPO}]^+$ respectively display bands at 445, 450, and 486 nm (Table 1). A time-dependent DFT (TD-DFT) approach identifies them as $^1\text{MLCT}$ transitions, with excitation of an electron from a Ru $d(\pi^*)$ orbital toward a π^* orbital centered on polypyridyl ligands. The important red shift for $[\text{RuPO}]^+$ is caused also by the weak π -acceptor ability of the PO ligand.

All of the complexes in Table 1 are luminescent at 77 K; however, only $[\text{RuP}(\text{N})]^{2+}$ and $[\text{RuPO}]^+$ are emissive at room temperature, and remarkably $[\text{RuPO}]^+$ alone presents a significant long-lived emission ($\tau = 57$ ns; $\Phi = 1.4 \times 10^{-3}$). This clearly shows that this PO ligand makes a difference in terms of the emission lifetime.

DFT calculations on the lowest triplet excited-state potential energy surface of $[\text{RuPO}]^+$, $[\text{RuP}(\text{N})]^{2+}$, and $[\text{RuPH}]^{2+}$ located, in each case, one $^3\text{MLCT}$ state minimum and one ^3MC state minimum. The $^3\text{MLCT}$ states are the emissive ones and are formed from the ground state by HOMO/LUMO transitions. The vertical emission energies calculated from these states and referred to as ΔSCF in Table 1 are only in modest agreement with the experimental values. Hence, we chose to move beyond this purely electronic picture by simulating a vibrationally resolved emission spectrum (VRES).¹¹ This procedure largely improves the agreement between calculated and experimental emission maxima (Table 1). Inclusion of an explicit methanol molecule in the vicinity of the PO ligand improves, furthermore, this agreement, showing that there is strong interaction between the PO group and solvent.

To investigate in more depth the factors responsible for the observation of luminescence at room temperature of $[\text{RuPO}]^+$, we performed calculations of the free-energy profiles connecting the $^3\text{MLCT}$ and ^3MC states for $[\text{RuPH}]^{2+}$, $[\text{RuP}(\text{N})]^{2+}$, and $[\text{RuPO}]^+$. As can be seen in Figure 3, two important facts reveal that $[\text{RuPO}]^+$ will not behave like the other two complexes. $[\text{RuPO}]^+$ is the only one having its ^3MC state above the $^3\text{MLCT}$ state and, furthermore, these two states are separated by a large barrier, which is not the case for the other two complexes. Thus, the ^3MC state of $[\text{RuPO}]^+$ is the most difficult to reach, and so room temperature luminescence from the $^3\text{MLCT}$ state is assured. It is worth noting that the intermediate photophysical behavior of $[\text{RuP}(\text{N})]^{2+}$, luminescent at room temperature but with a nondetectable emission lifetime, is easily intelligible from these profiles. $[\text{RuP}(\text{N})]^{2+}$ possesses a smaller $^3\text{MLCT} \rightarrow ^3\text{MC}$ activation energy barrier than that of $[\text{RuPO}]^+$ but a larger backward activation barrier. These two factors penalize the reverse $^3\text{MC} \rightarrow ^3\text{MLCT}$ conversion, explaining the nondetectable emission lifetime of $[\text{RuP}(\text{N})]^{2+}$. For $[\text{RuPO}]^+$, the small reverse activation energy can be easily overcome and accounts for the large emission lifetime of 57 ns. Thus, the key factors of the long-lived luminescent $^3\text{MLCT}$ state of $[\text{RuPO}]^+$ are destabilization of the ^3MC state and the lateness of its transition state, which are both due to the strong σ -donor properties of the anionic L-type phosphoryl ligand.

In conclusion, we report experimental evidence of a long-lived room temperature luminescent complex promoted by an organophosphoryl ligand coordinated on the $[\text{Ru}(\text{bpy})(\text{tpy})]^{2+}$ metal core. As suggested by ELF and NBO analysis, the phosphoryl fragment can be described as a strong σ -donor anionic P^{III} -type ligand. Free-energy profile calculations on the excited states revealed that both favorable thermodynamic and kinetic factors are responsible for the remarkable luminescence properties of the phosphoryl complex. Thus, incorporating organophosphorus ligands in ruthenium polypyridyl complexes induced a drastic change in their photophysical properties.¹² The next step in our studies will now consist of transposing our methodology to ruthenium bis(bipyridyl) complexes known for their superior photophysical properties over the $[\text{Ru}(\text{bpy})-(\text{tpy})]^{2+}$ metal core and to low-cost transition metals.¹³

Table 1. Selected Photophysical Data for [RuPPh]²⁺, [RuPH]²⁺, [RuPO]⁺, and [RuP(N)]²⁺ Complexes ([Ru] = Ru(tpy)(bpy), P = PPh₂, and (N) = N=C(H)N(i-Pr)₂ and PF₆⁻ as Counteranions)

		[RuPPh] ²⁺ ^a	[RuPH] ²⁺	[RuP(N)] ²⁺	[RuPO] ⁺
absorption					
exptl	λ_{abs} (nm)/ ϵ (L·mol ⁻¹ ·cm ⁻¹)	440/8000	445/6380	450/7250	486/10900
calcd	λ_{abs} / ϵ	421/15000	405/11000	420/10000	442/12000
emission					
77 K	λ_{em} (nm)/ τ (μ s)	615/5.0	594/6.3	619/4.8	646/2.8
298 K	λ_{em} (nm)/ τ (ns)			640/nd	698/57
calcd Δ SCF	λ_{em} (nm)		698	734	869
calcd VRES ^b	λ_{em} (nm)		656		747 ^b /775 ^c /725 ^d

^aSee ref 3b. ^b λ_{em} calculated (77 K) by simulating vibrationally resolved emission spectra. ^cEffects of the temperature on the emission energies (298 K) are reproduced by means of a Boltzmann distribution. ^d λ_{em} calculated (298 K) by simulating vibrationally resolved emission spectrum of [RuPO]⁺ plus an explicit methanol molecule in the vicinity of the PO unit (P=O---H---OCH₃).

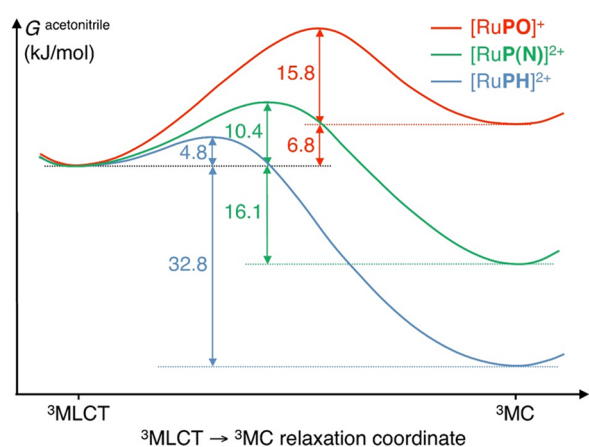


Figure 3. Schematic representation of the free-energy profiles computed with DFT in acetonitrile at 298 K for [RuPH]²⁺ (in blue), [RuP(N)]²⁺ (in green), and [RuPO]⁺ (in red). The ³MLCT states were deliberately placed at the same energy origin for clarity.

■ ASSOCIATED CONTENT

Supporting Information

Experimental procedures, characterization, electrochemical and photophysical analysis, and computational details. This material is available free of charge via the Internet at <http://pubs.acs.org>.

■ AUTHOR INFORMATION

Corresponding Authors

*E-mail: fabienne.alary@irsamc.ups-tlse.fr.

*E-mail: alain.igau@lcc-toulouse.fr.

Notes

The authors declare no competing financial interest.

■ ACKNOWLEDGMENTS

E.L. is grateful to Ministère de la Recherche for a PhD fellowship. R.S. is grateful to the ANR program for a PhD fellowship. Johnson Matthey is acknowledged for RuCl₃·xH₂O. This work was performed using HPC resources from CALMIP (Grant 2010-P0880).

■ REFERENCES

(1) (a) Campagna, S.; Puntoriero, F.; Nastasi, F.; Bergamini, G.; Balzani, V. *Top. Curr. Chem.* **2007**, *280*, 117. (b) Medlycott, E. A.; Hanan, G. S. *Coord. Chem. Rev.* **2006**, *250*, 1763. (c) Balzani, V.; Scandola, F. *Supramolecular Photochemistry*; Ellis Horwood: New York, 1991. (d) Meyer, T. J. *Pure Appl. Chem.* **1986**, *58*, 1193.

(2) (a) Zhao, Q.; Huang, C.; Li, F. *Chem. Soc. Rev.* **2011**, *40*, 2508. (b) Fernandez-Moreira, V.; Thorp-Greenwood, F. L.; Coogan, M. P. *Chem. Commun.* **2010**, *46*, 186. (c) Gill, M. R.; Garcia-Lara, J.; Foster, S. J.; Smythe, C.; Battaglia, G.; Thomas, J. A. *Nat. Chem.* **2009**, *1*, 662. (d) Zhu, Y.; Gu, C.; Tang, S.; Fei, T.; Gu, X.; Wang, H.; Wang, Z.; Wang, F.; Lu, D.; Ma, Y. *J. Mater. Chem.* **2009**, *19*, 3941. (e) Evans, R. C.; Douglas, P.; Winscom, C. J. *Coord. Chem. Rev.* **2006**, *250*, 2093. (f) Slinker, J.; Bernards, D.; Houston, P. L.; Abruña, H. D.; Bernhard, S.; Malliaras, G. G. *Chem. Commun.* **2003**, 2392. (g) Clifford, J. N.; Martinez-Ferrero, E.; Viterisi, A.; Palomares, E. *Chem. Soc. Rev.* **2011**, *40*, 1635. (h) Nazeeruddin, M. K.; Grätzel, M. *Struct. Bonding (Berlin)* **2007**, *123*, 113.

(3) (a) Lebon, E.; Bastin, S.; Sutra, P.; Vendier, L.; Piau, R. E.; Dixon, I. M.; Boggio-Pasqua, M.; Alary, F.; Heully, J.-L.; Igau, A.; Juris, A. *Chem. Commun.* **2012**, *48*, 741. (b) Dixon, I. M.; Lebon, E.; Loustau, G.; Sutra, P.; Vendier, L.; Igau, A.; Juris, A. *Dalton Trans.* **2008**, 5627.

(4) (a) Smith, R. C.; Earl, M. J.; Protasiewicz, J. D. *Inorg. Chim. Acta* **2004**, *357*, 4139. (b) Yamaguchi, S.; Akiyama, S.; Tamao, K. *J. Organomet. Chem.* **2002**, *646*, 277. (c) Fukazawa, A.; Hara, M.; Okamoto, T.; Son, E.-C.; Xu, C.; Tamao, K.; Yamaguchi, S. *Org. Lett.* **2008**, *10*, 913. (d) Stolar, M.; Baumgartner, T. *New J. Chem.* **2012**, *36*, 1153.

(5) (a) Chesnut, D. B. *J. Phys. Chem. A* **2003**, *107*, 4307. (b) Chesnut, D. B.; Savin, A. *J. Am. Chem. Soc.* **1999**, *121*, 2335. (c) Gilheany, D. G. *Chem. Rev.* **1994**, *94*, 1339 and references cited therein.

(6) Pavlik, S.; Mereiter, K.; Puchberger, M.; Kirchner, K. *Organometallics* **2005**, *24*, 3561.

(7) Becke, A. D.; Edgecombe, K. E. *J. Chem. Phys.* **1990**, *92*, 5379. Silvi, B.; Savin, A. *Nature* **1994**, *371*, 683.

(8) Reed, A. E.; Curtiss, L. A.; Weinhold, F. *Chem. Rev.* **1988**, *88*, 899.

(9) Abdellah, I.; Bernoud, E.; Lohier, J. F.; Alayrac, C.; Toupet, L.; Lepetit, C.; Gaumont, A. C. *Chem. Commun.* **2012**, *48*, 4088.

(10) The MPWB1K and B3LYP functionals were chosen on the basis of their performances with Ru(II) polypyridyl complexes containing P-ligands. All calculations were performed with a large basis set made of a polarized double- ζ basis set for H atoms, a polarized triple- ζ basis set for C, N, and P atoms, and a Stuttgart relativistic small-core effective potential for Ru atoms with its associated basis set including one f polarization function with an exponent of 0.96.

(11) Petrenko, T.; Neese, F. *J. Chem. Phys.* **2007**, *127*, 164319(1–15).

(12) Litke, S. V.; Ershov, A. Y.; Meyer, T. J. *J. Phys. Chem. A* **2011**, *115*, 14235. Kinoshita, T.; Dy, J. T.; Uchida, S.; Kubo, T.; Segawa, H. *Nat. Photon.* **2013**, *7*, 535.

(13) For Fe^{II}-based dyes in photovoltaics, see: Liu, Y.; Harlang, T.; Canton, S. E.; Chäbera, P.; Suàrez-Alcàntara, K.; Fleckhaus, A.; Vithanage, D. A.; Göransson, E.; Corani, A.; Lomoth, R.; Sundström, V.; Wärnmark, K. *Chem. Commun.* **2013**, *49*, 6412. Ferrere, S.; Gregg, B. A. *J. Am. Chem. Soc.* **1998**, *120*, 843 and references cited therein.